

## Diamond machining of sinusoidal grid surface using fast tool servo system for fabrication of hydrophobic surface

Hong LU<sup>1</sup>, Deug-Woo LEE<sup>2</sup>, Sang-Min LEE<sup>1</sup>, Jeong-Woo PARK<sup>3</sup>

1. Department of Nano Fusion Technology, Pusan National University, Miryang 627-706, Korea;
2. Department of Nano Mechatronics Engineering, Pusan National University, Miryang 627-706, Korea;
3. Department of Mechanical Design Engineering, Chosun University, Gwangju 501-759, Korea

Received 21 May 2012; accepted 27 September 2012

**Abstract:** Ultra-precision diamond machining with piezoelectric-assisted fast tool servo (FTS) was used to produce various free-form surfaces. A low cost, rapid and large area fabrication of uniform hydrophobic surface at room temperature which transfers the FTS fabricated sinusoidal grid surface to the flat film with UV-moulding process was described. A piezoelectric-assisted FTS with high band width of 2 kHz, travel range up to 16  $\mu\text{m}$  and the compact mechanism structure was designed for the sinusoidal grid surface machining and the dynamic performance testing of FTS was described in detail. Machining results indicate that the dimensions of sinusoidal grid change with the variation of the FTS machining condition. Wetting properties of UV-moulded surface were evaluated, the best contact angle was measured to be 120.5° on the sinusoidal grid surface with profile wavelength of 350  $\mu\text{m}$  and peak-to-valley amplitude of about 16  $\mu\text{m}$ .

**Key words:** fast tool servo system; diamond turning; sinusoidal grid surface; UV-moulding; contact angle

### 1 Introduction

Precision diamond turning technology with fast tool servo system (FTS) was extensively developed for the fabrication of freeform optical surfaces [1-3]. This technique requires tool driven at a frequency evidently higher than the rotational frequency of the spindle. However, the standard slide actuators cannot meet this requirement due to their large mass and consequent low natural frequency. Therefore, a stacked piezoelectric actuator become necessary, which has a relatively short maximum travel range less than 100  $\mu\text{m}$  and high frequency limited by either structural resonance or power amplifier limitation. RASMUSSEN et al [4] designed a piezoelectric-driven cutting tool system capable of dynamically controlling depth of cut that can be used to machine slightly non-circular workpieces. With an amplification mechanism, the tool was able to produce 52  $\mu\text{m}$  travel range with frequency of 200 Hz. Tool motion error less than 0.5  $\mu\text{m}$  was achieved using a repetitive controller. The same device was proposed to be used for an active damping element for improving the

surface finish. DOW et al [5] designed a FTS utilized a piezoelectric ring type attack actuator (out diameter 25 mm, length 18 mm, free stroke 20  $\mu\text{m}$ ) and a pair of high-bandwidth capacitive sensors. The unit produced approximately 5  $\mu\text{m}$  of full stroke at 1 kHz with a usable bandwidth of over 2 kHz. This research also revealed that the dynamic thrust forces caused by cutting had little effect on the quality of the finished surface. KIM and KIM [6] designed a FTS for diamond turning of flat surface. The FTS can follow the command input sine wave with amplitude of 7.5  $\mu\text{m}$  and frequency up to 100 Hz effectively, and the peak-to-valley error level is 0.15  $\mu\text{m}$ . Most of these FTSs, which are designed for special machine tools and special tasks, do not satisfy our demands for machining microstructure surface because of short stroke, inferior precision and low bandwidth.

Usually, the more complex microstructure surfaces require the FTS to provide with the frequency performance increasing. Therefore, in this case, the lowest frequency of the FTS must be larger than 1 kHz, and the higher the better if other requirements are satisfied. Furthermore, the UV-moulding process was utilized to transfer the machined microstructure to the

plane film. This process provides the components with low thermal expansion, enhanced stability and low birefringence, and can be applied to replicating optical components with very small features [7–11].

The machining evaluation of a novel FTS was used to fabricate sinusoidal grid surface on the brass roller, then transfer the microstructure to the plane film with the UV-moulding process. A piezoelectric-assisted FTS with high band width of 2 kHz, travel range up to 15  $\mu\text{m}$  and the compact mechanism structure was designed. A function generator provided the command signals to the FTS, the signals were magnified by a high power amplifier. All actual machining tests were performed on a roller machine. The machining results indicate that the dimensions of sinusoidal grid change with the variation of the FTS machining condition. The wetting properties of the UV-moulded sinusoidal grid surface were evaluated by measuring the static contact angles for each sample. In this research, the best contact angle was measured to be 120.5° on the sinusoidal grid surface with profile wavelength of 350  $\mu\text{m}$  and peak-to-valley amplitude of about 16  $\mu\text{m}$ . The actual fabrication result of the sinusoidal microstructure indicates the effectiveness of the designed FTS system.

## 2 Design and basic characteristics of FTS

The general structure of the FTS designed in this investigation is shown in Fig. 1. The FTS is composed of a main body base, a tool holder adhered to the moving body and a piezoelectric actuator. The mechanical structure is made of aluminium alloy. The moving portion of the FTS is guided by a set of leaf spring, which is bolted to the main body base. The symmetry structure in the design can inherently balance the flexure mechanism and avoid coupled interference motion. The piezoelectric actuator is stocked type with 31 mm in length and 10 mm in outer diameter, which is preloaded by a pretightening nut. The preload mechanism ensures

that the piezoelectric actuator is never under tensile stress, which may damage the actuator.

For the performance testing of the FTS, a test system was built using a LabVIEW computer, a high voltage amplifier, a capacitive sensor and a high-speed data acquisition. The driving signal is amplified 100 times to produce the voltage signal to drive the piezoelectric actuator in the desired direction through the high voltage amplifier. In order to acquire the signal from the capacitive displacement sensor, two A/D channels were used when their speeds were set to 20 kHz for one cycle control of execution in the computer. In order to reduce the external disturbance, such as vibration, the experiments were carried out on a passive micro-vibration table. The environmental noise after the passive micro-vibration system is approximately 3 nm.

The hysteresis curve of FTS is obtained by applying increasing and then decreasing voltage of 25 V intervals from 0 to 150 V to the piezoelectric actuator, as shown in Fig. 2. The lower curve represents the expansion process and the upper curve represents the retraction process. When a 150 V control signal is applied to the piezoelectric actuator, the maximum displacement of the FTS is approximately 43.2  $\mu\text{m}$ . A significant hysteresis characteristic is observed in this figure. This is due to the crystalline polarization effects of the piezoelectric material in open-loop operation. Usually, this hysteresis phenomenon can be reduced by using closed-loop control with displacement feedback, and the linearity of the FTS can be improved.

High resolution of the FTS is a necessary performance for the high precision machining. Therefore, the resolution of the FTS must be of the order of nanometre to manufacture microstructure surface with submicron-form accuracy and nanometre roughness.

A stair control voltage with the value of 0.2 V was applied to the amplifier of the actuator, and the displacement of FTS was recorded by the capacitive sensor. The resolution of the FTS is shown in Fig. 3. It

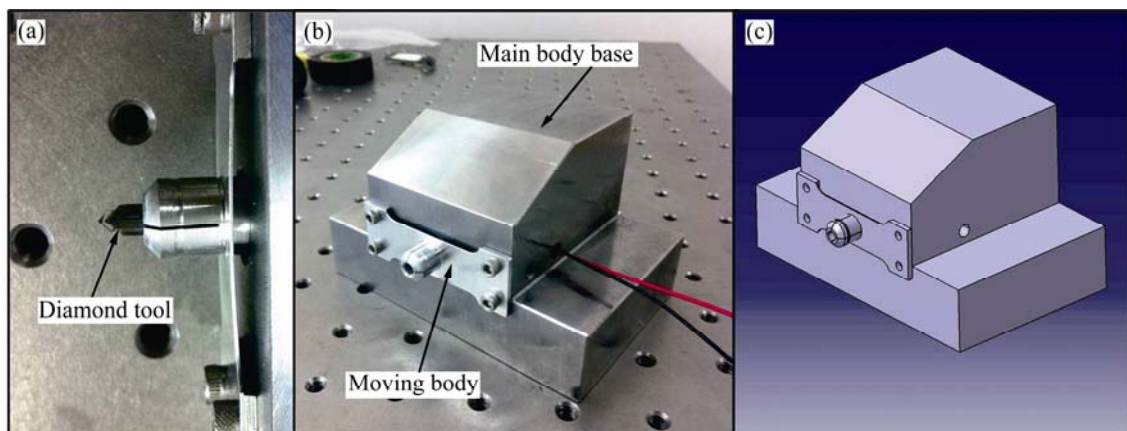


**Fig. 1** Photographs of diamond tool and tool holder (a), FTS front face (b) and schematic diagram of FTS (c)

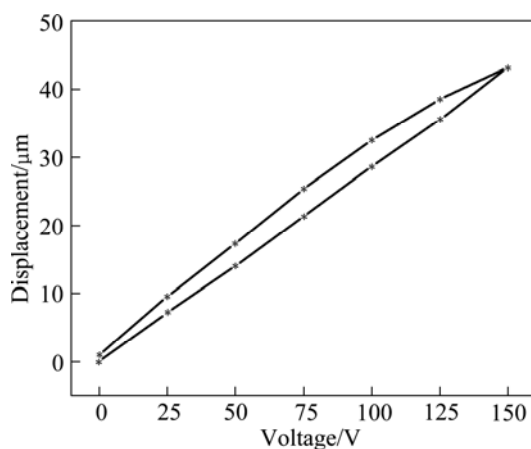


Fig. 2 Hysteresis of FTS (open-loop)

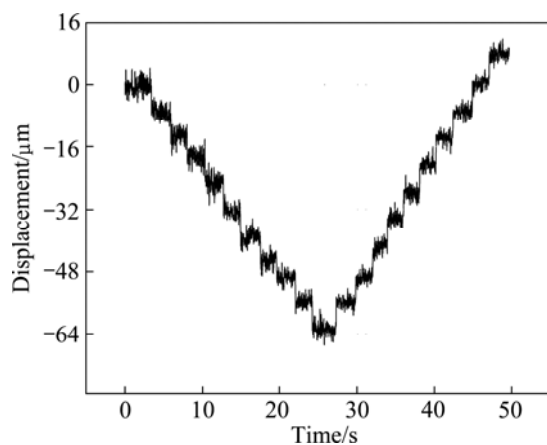


Fig. 3 Step wise response of FTS

can be seen that the resolution of FTS can reach up to 8 nm. In fact, a high resolution can be obtained if the environmental noise can be strictly controlled to a minimum level.

### 3 Fabrication and discussion

#### 3.1 Fabrication of master roller

Figure 4 shows the photo of the turning machine used for the fabrication of the sinusoidal microstructure in this investigation. The machine is composed of three main parts: the aerostatic spindle and tailstock to rotate the roller, an  $x$ -axis linear servo to laterally move the diamond tool along the roller for providing the feed rate, and a  $y$ -axis linear servo to translate the diamond tool for generating depth profile. The machining process of FTS is shown in Fig. 5. A copper alloy specimen with length of 1.5 m and diameter of 170 mm is clamped on the spindle. FTS is fixed on the feed guide of machine. The function generator produces the desired diamond tool motion trajectory that is sent to the amplifier as the reference input of the FTS. The cutting tool is driven by the FTS cut into and out of the workpiece several times

per revolution along the  $y$ -axis direction. The quality of machined microstructures was evaluated by an optical microscopy and an alpha-step.

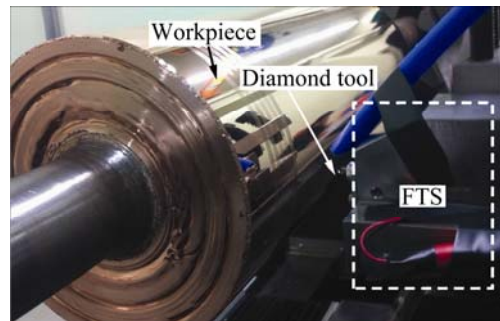


Fig. 4 Photo of FTS attached to roll machine

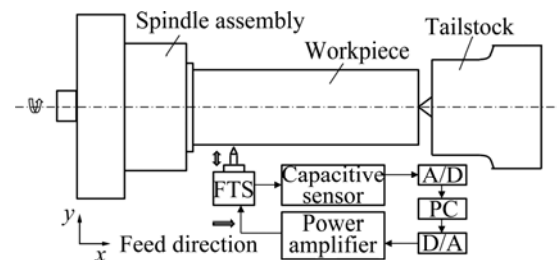


Fig. 5 Machining process of FTS

#### 3.2 UV-moulding and evaluation of sinusoidal grid surface

A UV-moulding technique was performed to replicate the profile of the microstructure on a plane. The UV-moulding provided a high degree of accuracy and could be achieved at room temperature and low pressures [7]. According to a UV resin in the liquid state between the workpiece and the plastic film, and UV light was applied above the plastic film. The profile of the microstructure was moulded on the film with the UV resin curing, as shown in Fig. 6.

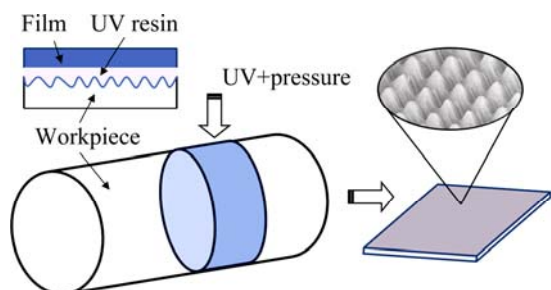
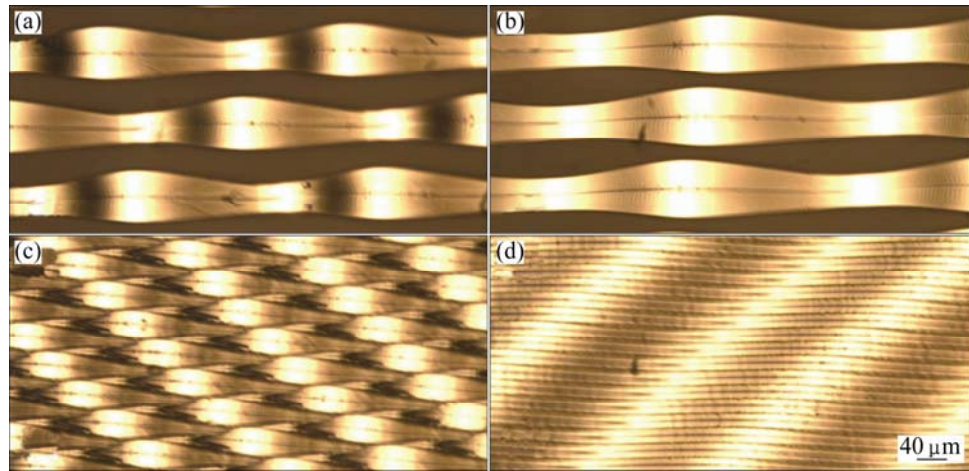


Fig. 6 UV-moulding process

Figure 7 shows four optical micro graphs of the resultant microstructure at low magnification. In both cases, the tool has been excited by a sinusoidal oscillation with the frequency of 500–2000 Hz. The microstructures in Figs. 7(a) and (b) were generated with the feed rate of 100  $\mu\text{m}/\text{r}$ , driving frequency of 1500 Hz



**Fig. 7** Optical microscope photographs of microstructure with driving frequency of 1.5 kHz at different spindle speeds and feed rates: (a) 57 r/min, 100  $\mu\text{m}/\text{r}$ ; (b) 72 r/min, 100  $\mu\text{m}/\text{r}$ ; (c) 57 r/min, 20  $\mu\text{m}/\text{r}$ ; (d) 72 r/min, 20  $\mu\text{m}/\text{r}$

and the spindle speed of 57 r/min and 72 r/min, respectively. Each single microstructure is clearly distinguishable and is free of breakages. The structured surfaces in Figs. 7(c) and (d) were produced using same excitation signal as the Figs. 7(a) and (b). And the feed rate is 20  $\mu\text{m}/\text{r}$ , the spindle speeds are 57 r/min and 72 r/min, respectively. In Fig. 7(a), for the contiguous two grooves, the peak of one groove is next to the valley of the other groove. Therefore, the valley array is clearly identified when the feed rate decreases and the grooves overlay each other, as shown in Fig. 7(c). However, the grooves distribution of Fig. 7(b) is opposite from the grooves distribution that shown in Fig. 7(a). Thus, the sinusoidal corrugated surface is generated, as shown in Fig. 7(d). This result shows that the configuration of the finished surface will transform as the machining conditions changes.

An alpha-step with the scan length up to 1 mm was used to evaluate the profile quality of the machined microstructure, as shown in Fig. 8. At the bottom of the height maps, the profile curve through one of the structure is shown. Its position is marked in the height map with a dashed line. From the profile graph, it is obvious that the wave length of the profile is defined by three factors: the spindle speed, the radius of roller and the driving frequency of FTS, and it can be calculated by following equation:

$$\lambda = \frac{v}{60} \times 2\pi r \times \frac{1}{f} \quad (1)$$

where  $\lambda$  is the wave length of profile,  $v$  is the spindle speed,  $r$  is the radius of the roller, and  $f$  is the driving frequency of FTS. With the spindle speed of 57 r/min and the driving frequency of 1500 Hz,  $\lambda$  is determined to be 340  $\mu\text{m}$  in Fig. 8(a). This value has a great agreement with the actual measured value. In terms of

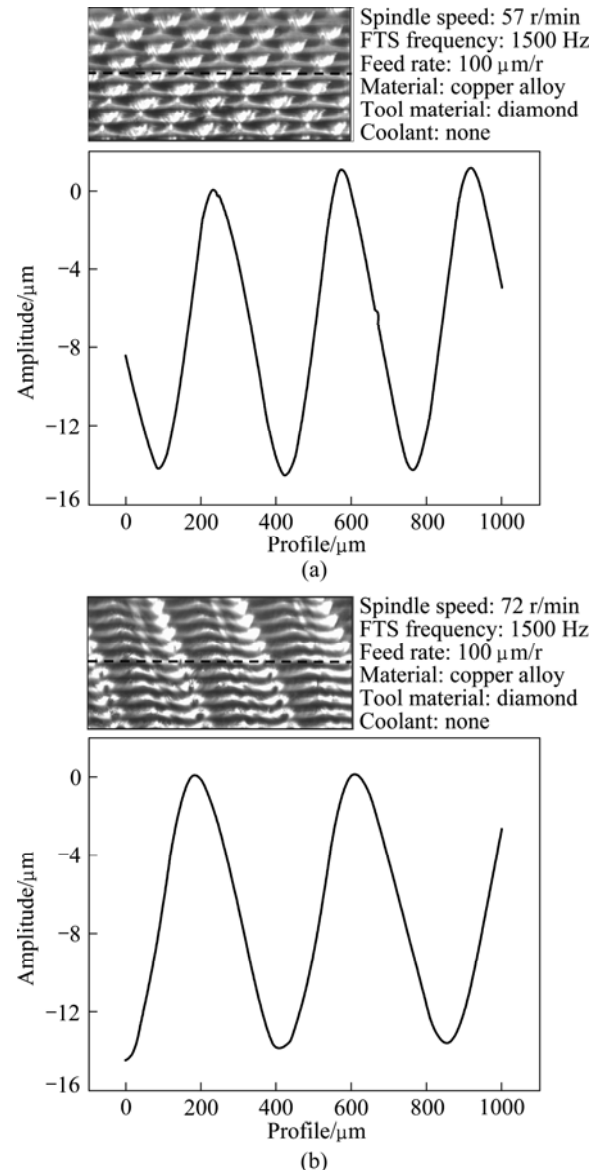


**Fig. 8** Surface height map and profile generated with different spindle speeds: (a) 57 r/min; (b) 72 r/min

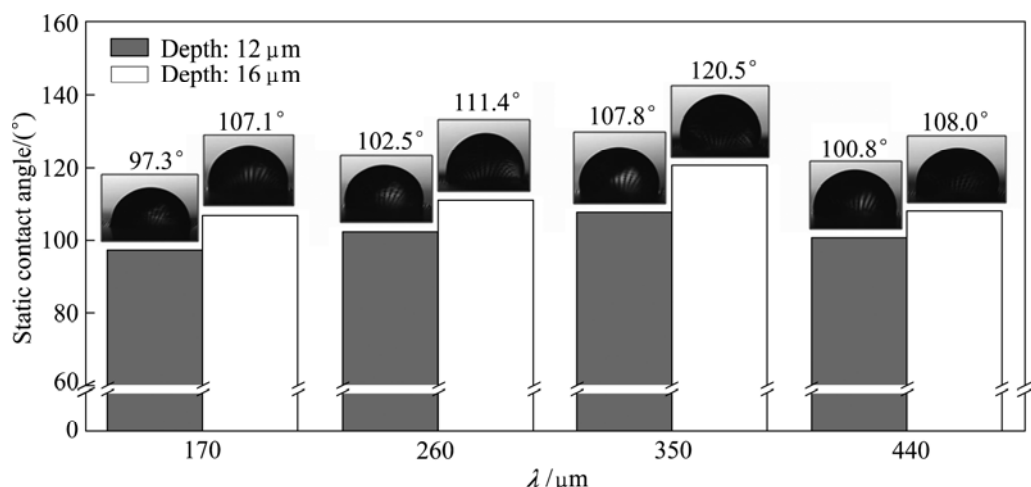


**Fig. 9** Measured static contact angle of UV-moulded sinusoidal grid surface (Insert figures are water droplets on each sample captured during measuring)

bandwidth, this FTS can be capable of following a trajectory of sinusoidal shape with 1500 Hz and spindle rotating at 57 r/min, there are about 1500 repeating peaks and valleys in one revolution. The structured surface in Fig. 8(b) is produced using the same excitation signal as Fig. 8(a) with the spindle speed of 72 r/min. The wavelength of profile in Fig. 8(b) is distinctly greater than that shown in Fig. 8(a) because of the increase of the spindle rotation.

### 3.3 Measurement of static wetting property of UV-moulded sinusoidal grid surface

The wetting properties of the UV-moulded sinusoidal grid surface were evaluated by measuring the static contact angles (CAs) for each sample. In all measurements, a volume of the water droplet was fixed to be 10  $\mu\text{L}$ , and the measurements were performed on the two group of UV-moulded sinusoidal grid sample with the peak-to-valley amplitude of 12  $\mu\text{m}$  and 16  $\mu\text{m}$ , respectively, as shown in Fig. 9. In order to compare the two groups of samples, the structured surface with peak-to-valley amplitude of 16  $\mu\text{m}$  provided greater CA than the others. And the static CAs were increased gradually with increasing the profile wavelength ( $\lambda$ ) of the structured surface up to 350  $\mu\text{m}$ , and the best CA was measured to be 120.5° on the sample with  $\lambda$  of 350  $\mu\text{m}$  and the peak-to-valley amplitude of 16  $\mu\text{m}$ .

However, the CA was lower on the sample of  $\lambda=440$   $\mu\text{m}$  because the increase of distance between every two peaks led the structured surface to flatten. These results clearly reveal that the process concept of a sinusoidal grid surface, which is based on the FTS machining and UV-moulding technique, can be realized in a simple and low cost large area fabrication of uniform hydrophobic surface at room temperature.

## 4 Conclusions

- 1) The resolution of FTS can reach up to 8 nm with a stair control voltage of 0.2 V.
- 2) The machined configuration depended on three factors: spindle speed, FTS driving frequency and radius of roller. The calculation method of sinusoidal grid dimensions was reported.
- 3) The wetting properties of the UV-moulded sinusoidal grid surface were evaluated. The best contact angle was measured to be 120.5° with the sample profile wavelength of 350  $\mu\text{m}$  and peak-to-valley amplitude of about 16  $\mu\text{m}$ .
- 4) A large area sinusoidal grid surface on a roller with the diameter of 300 mm and length of 2 m will be fabricated by this FTS. The feedback control of tool is positioned by adding a displacement sensor.

## Acknowledgement

This work was supported by NCRC (National Core Research Center) program of the Ministry of Education, Science and Technology (2010-0008-277) and “Development of next generation multi-functional machining systems for eco/bio components” project of ministry of knowledge economy.

## References

- [1] RAKUFF S, CUTTINO J F. Design and testing of a long-rang precision fast servo system for diamond turning [J]. Precision Engineering, 2009, 33: 18–25.
- [2] KIM J D, KIM D S. Waviness compensation of precision machining by piezoelectric micro cutting device [J]. Journal of Machine Tool & Manufacture, 1998, 38: 1305–1322.

- [3] MAO H, HU D, ZHANG K. A fast tool feeding mechanism using piezoelectric actuators in noncircular turning [J]. International Journal of Advanced Manufacturing Technology, 2005, 27: 254–259.
- [4] RASMUSSEN J D, TSAO T C, HANSON R D, KAPOOR S G. Dynamic variable depth of cut machining using piezoelectric actuators [J]. Journal of Machine Tool & Manufacture, 1994, 34(3): 379–392.
- [5] DOW T A, MILLER M H, FALTER P J. Application of a fast tool servo for diamond turning of nonrotationally symmetric surface [J]. Precision Engineering, 1991, 13(4): 243–250.
- [6] KIM H S, KIM E J. Feed forward control of fast tool servo for real time correction of spindle error in diamond turning of flat surface [J]. Journal of Machine Tool & Manufacture, 2003, 43: 1177–1183.
- [7] KIM S, KANG S. Replication qualities and optical properties of UV-moulded microlens arrays [J]. Journal of Physics D: Applied Physics, 2003, 36(20): 2451–2456.
- [8] TANIGAMI N, OGATA S, AOYAMA S, YAMASHITA T, IMANAKA K. Low wavefront aberration and high-temperature stability molded micro Fresnel lens [J]. IEEE Photon Technol Lett, 1989, 11(1): 384–385.
- [9] BRAUN A, ZIMMER K, HOSSELBARTH B, MEINHARDT J, BIGL F, MEHNERT R. Excimer laser micromachining and replication of 3D optical surfaces [J]. Appl Surf Sci, 1998, 127–129: 911–914.
- [10] RUDSCHUCK S, HIRSCH D, ZIMMER K, OTTE K, BRAUN A, MEHNERT R, BIGL F. Replication of 3D-micro- and nanostructures using different UV-curable polymers [J]. Microelectron Eng, 2000, 53: 557–560.
- [11] TING C J, CHANG F Y, CHEN C F, CHOU C P. Fabrication of an antireflective polymer optical film with subwavelength structures using a roll-to-roll micro-replication process [J]. J Micromech Microeng, 2008, 18: 075001.

(Edited by LI Yan-hong)